Physics Letters B 772 (2017) 529–533

Contents lists available at ScienceDirect

Physics Letters B

www.elsevier.com/locate/physletb

Northern boundary of the "island of inversion" and triaxiality in ^{34}Si

R. Han [a], X.Q. Li [a,1], W.G. Jiang [a], Z.H. Li [a,*], H. Hua [a,*], S.Q. Zhang [a], C.X. Yuan [b], D.X. Jiang [a], Y.L. Ye [a], J. Li [a], Z.H. Li [a], F.R. Xu [a], Q.B. Chen [a], J. Meng [a], J.S. Wang [c], C. Xu [a], Y.L. Sun [a], C.G. Wang [a], H.Y. Wu [a], C.Y. Niu [a], C.G. Li [a], C. He [a], W. Jiang [a], P.J. Li [a], H.L. Zang [a], J. Feng [a], S.D. Chen [a], Q. Liu [a], X.C. Chen [a], H.S. Xu [c], Z.G. Hu [c], Y.Y. Yang [c], P. Ma [c], J.B. Ma [c], S.L. Jin [c], Z. Bai [c], M.R. Huang [c], Y.J. Zhou [c], W.H. Ma [c], Y. Li [c], X.H. Zhou [c], Y.H. Zhang [c], G.Q. Xiao [c], W.L. Zhan [c]

[a] School of Physics and State Key Laboratory of Nuclear Physics and Technology, Peking University, Beijing 100871, China
[b] Sino-French Institute of Nuclear Engineering and Technology, Sun Yat-Sen University, Zhuhai 519082, China
[c] Institute of Modern Physics, Chinese Academy of Sciences, Lanzhou 730000, China

ARTICLE INFO

Article history:
Received 27 March 2017
Received in revised form 16 June 2017
Accepted 5 July 2017
Available online 12 July 2017
Editor: D.F. Geesaman

Keywords:
Island of inversion
β-decay
Half-life
Triaxiality
Shell model

ABSTRACT

β-decay studies of neutron-rich nuclei in and around the "island of inversion" have been performed. With a systematic investigation of half-lives for the isotonic chains from $N = 19$ to 22, conspicuous kinks observed at $Z = 13$ provide a clear signature of a boundary on the northern (high-Z) side of the island. Based on the comparison with shell model calculations using Gogny D1S and SDPF-M interactions, a newly determined 2_2^+ state in ^{34}Si at 4519 keV presents an experimental evidence of triaxiality in this region and sheds more light on the structure of the transition across the northern boundary of the island.

Since the pioneering works on the shell structure in nuclei by Goeppert-Mayer [1] and Jensen et al. [2], magic numbers have played a major role in our understanding of nuclear structure close to β-stability. A nucleus with a magic number of nucleons shows signs of stability such as a spherical ground state and remarkably higher $E(2_1^+)$ energies and smaller $B(E2)$ values than their neighbors. With nuclear physics studies moving towards nuclei far from β-stability, such a picture was firstly broken in the light neutron-rich nuclei. In 1975, Thibault et al. [3] observed anomalous ground state properties in ^{31}Na deviating strongly from the prediction of the traditional shell model. Later on, more studies revealed a region of large deformation around $N = 20$, $Z < 14$ [4–8] and interpreted these anomalies as the reduction of the $N = 20$ shell gap, which is a result of the intrusion of neutron orbits from the pf shell into the sd shell. Warburton et al. [9] predicted that nuclei with this inversed ground states would constitute a 3×3 square with $Z = 10 \sim 12$, $N = 20 \sim 22$, which was referred to as the "island of inversion".

In the following years, uncovering the underlying inversion mechanism and exploring the scope of the island has been the focus of intensive theoretical and experimental investigations. The reduction of $N = 20$ shell gap is now known to be most likely caused by the strong nucleon–nucleon tensor interaction [10–13] and the original border of the "island of inversion" has been extended considerably [14–22]. The nuclei ^{29}F [14], ^{28}Ne [15], ^{29,30}Na [16–19], ^{31,35,36}Mg [20–22], which were originally outside the island, have been experimentally confirmed to be inside the island recently. Based on these achievements, now many attentions are focused on the further question about how this structure transition moves along the isotonic or isotopic chains: sharp or gradual? The answer to this question will provide a stringent test of various model predictions. For a better description of this structure transition, theory suggested that the triaxial degree of freedom plays an important role in this particular region [23–30]. However, due to the limited experimental spectroscopic information available in this region, there is yet no decisive evidence of triaxiality to date.

* Corresponding authors.
E-mail addresses: zhli@pku.edu.cn (Z.H. Li), hhua@pku.edu.cn (H. Hua).
[1] X.Q. Li contributed equally to this work.

http://dx.doi.org/10.1016/j.physletb.2017.07.007

In this Letter, we report on a systematic study of the β-decay properties of nuclei in this region to explore the inversion character on the northern (high-Z) side of the island and to search for experimental evidence of triaxiality. To study the properties of extremely neutron-rich nuclei, β-decay has served as an important spectroscopic tool. With the advances in radioactive ion beam and β detection technologies, systematic β-decay studies of a number of neutron-rich nuclei are now possible in one experiment. They provide a sensitive probe to elucidate the trends of nuclear structure. In the present work, with the systematic investigation of half-lives for the isotonic chains from $N = 19$ to 22, conspicuous kinks are observed at $Z = 13$, which provide a clear signature of a boundary on the northern side of the island. Meanwhile, detailed β-delayed γ-spectroscopic study of the boundary nucleus ^{34}Al presents experimental evidence of triaxiality in ^{34}Si, which is helpful for a comprehensive understanding of the structure transition across the northern boundary of the island.

The β-decay experiment was carried out at Radioactive Ion Beam Line in Lanzhou (RIBLL) [31]. The primary beam ^{40}Ar at 69.2 MeV/nucleon, which was provided by the Heavy Ion Research Facility in Lanzhou (HIRFL), was impinged on a ^{9}Be target with a thickness of 182.6 mg/cm^2 to produce the neutron-rich radioactive species around the $Z \sim 12$, $N \sim 20$ region. The magnetic rigidity selection at RIBLL was optimized for the radioactive nucleus ^{34}Al and the radioactive ions were identified by the combination of energy loss (ΔE), time-of-flight (TOF), and magnetic rigidity (Bρ) on an event-by-event basis at RIBLL. Passing through a thin kapton window (25 μm thick), which separated the vacuum of the beam line from the air, and a stack of aluminum degraders, the radioactive ions were finally transported into the target chamber filled with low-temperature nitrogen and implanted in a 1500 μm-thick double-side Si strip detector (DSSD) of 50×50 mm^2. The experiment was performed in the continuous beam mode, which has a higher beam efficiency compared to the traditional beam-on/off mode [32,33]. By correlating the implanted nuclei with their subsequent β-particles within the same pixel or adjacent pixels of the DSSD, the β-decay properties of the implanted nuclei could be measured with much less disturbance from other unstable nuclei and the random background [34]. The DSSD was situated between two 3000 μm-thick plastic scintillators, one of which was used for beam diagnostics while the other was used as a veto detector, as well as for the fast timing signals of β particles. The β-delayed γ-rays were detected by two Ge clover detectors located at 45 mm on the left- and right-hand sides of the beam axis around the implantation and β detection system. The γ detection efficiency was found to be 4.4% at ∼1 MeV and 1.6% at ∼3.3 MeV.

The decay curve was constructed for each nuclide by measuring the time difference between neutron-rich nuclei implantations and subsequent β particles. Fig. 1(a)–1(d) show the examples of β-decay curves for ^{30}Na, ^{32}Mg, ^{35}Al, and ^{36}Si, respectively. The half-lives measured in this work are given in Table 1 in comparison with the literature values. The overall agreement is good and improvements in measurement accuracy are achieved for ^{29,30}Na, ^{30,31,32}Mg, and ^{36,37}Si. Since the magnetic rigidity selection at RIBLL was optimized for the nucleus ^{34}Al in the present experiment, reliable half-lives of more neutron-rich isotopes in this region could not obtained. With the experimental half-lives obtained in the present experiment and those previously known, a systematic survey of half-lives in this region has been made. Fig. 2(a) displays the experimental half-lives as a function of the proton number Z for four isotonic chains from $N = 19$ to 22. Generally, for each of the isotonic chains, the half-lives of the isotones increase gradually with increasing of proton number Z (heading towards the β-stability). One intriguing feature observed in Fig. 2(a) is the presence of conspicuous kinks at $Z = 13$ in all four isotonic chains,

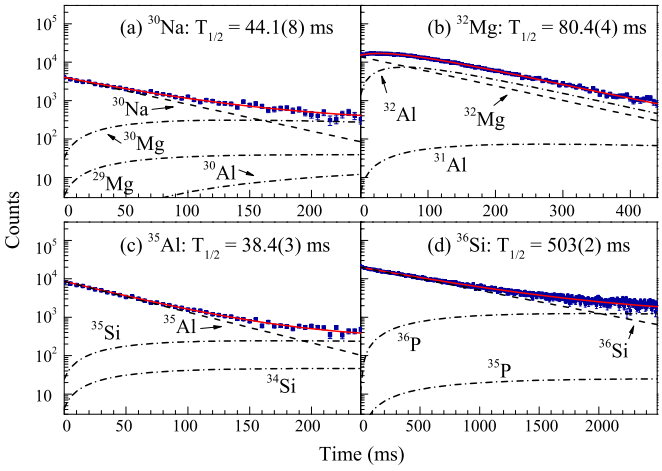

Fig. 1. (Color online). Fitted decay curves for (a) ^{30}Na, (b) ^{32}Mg, (c) ^{35}Al, and (d) ^{36}Si. Red solid line: the total decay curve; Dashed line: decay curve of implanted nuclei; Dot-dashed line: decay curves of the daughter and granddaughter nuclei.

Table 1
Experimental half-lives measured in this work in comparison with the literature values, which are taken from the National Nuclear Data Center [35] unless otherwise stated. All times are given in milliseconds.

A, Z	This work	Literature	A, Z	This work	Literature
^{27}Ne	29.3(21)	31.5(13)	^{32}Mg	80.4(4)	86(5)
^{28}Ne	19.2(6)	20(1)	^{33}Mg	93.9(18)	90.5(16)
^{28}Na	34.6(10)	30.5(4)	^{32}Al	31.7(3)	33.0(2)
^{29}Na	42.8(5)	44.1(9)	^{33}Al	41.4(1)	41.7(2)
^{30}Na	44.1(8)	48(2)	^{34}Al	51.5(9)	54.4(5) [36]
^{31}Na	16.6(4)	17.35(40)	^{35}Al	38.4(3)	37.2(8)
^{30}Mg	311(8)	335(17)	^{36}Si	503(2)	450(60)
^{31}Mg	270(2)	236(20)	^{37}Si	150(7)	90(60)

which obviously deviate from the systematics of the odd-even Z dependence.

To elucidate the origin of these kinks, shell-model calculations have been performed in the sd-$p_{3/2}f_{7/2}$ model space using the NUSHELLX code [37,38] with two interactions: the Gogny D1S interaction [39–42] and the SDPF-M interaction [43,44]. Both the interactions allow particle-hole excitations from the sd shell to the pf shell. In shell model calculations, there are always difficulties in dealing with the cross-shell nuclei because it is a difficult task to obtain reliable cross-shell matrix elements. The Gogny force is a unified interaction, which has been widely used in mean-field calculations. It can provide a consistent set of TBME in various model spaces without fitting the experimental data and therefore deal with the difficulties of cross-shell interactions effectively. The SDPF-M interaction, which has successfully been applied to describe the nuclear structure properties in and around the island of inversion [43,44], consists of three parts: the USD interaction [45] for the sd-shell, the Kuo–Brown interaction [46] for the pf-shell, and the modified Millener–Kurath interaction [47] for crossing the shells. The mixing between normal $0p$-$0h$ and intruder np-nh configurations is included in the present shell-model calculations without any restrictions. In comparison with the available experimental data, both the calculations give a good description to the ground states and low-lying excited states of nuclei in this region, and a good prediction of their configurations [48]. The calculated half-lives using the Gogny D1S and SDPF-M interactions are plotted in Fig. 2(b) in comparison with the experimental values of the $N = 19 \sim 22$ isotonic chains. It can be seen that both calculated re-

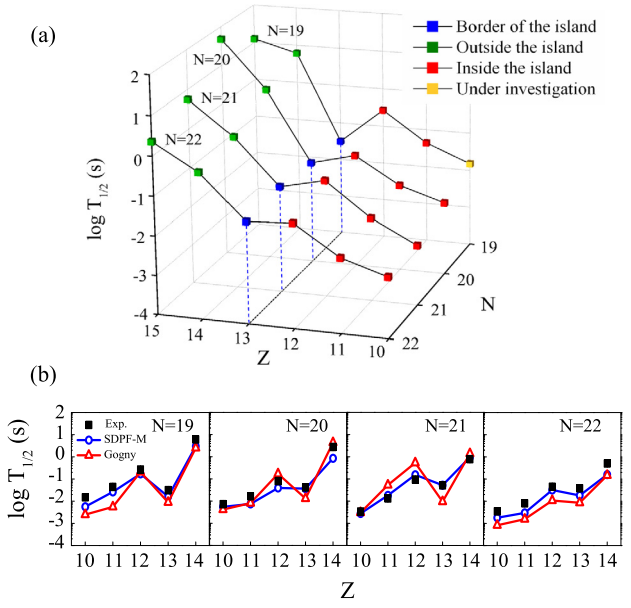

Fig. 2. (Color online). (a) Experimental half-lives of four isotonic chains from $N = 19$ to 22 in and around the "island of inversion". Data are taken from the present work and Refs. [35,53], respectively. (b) The theoretical half-lives of four isotonic chains obtained by shell model calculations with the Gogny D1S and the SDPF-M interactions are compared with experimental data.

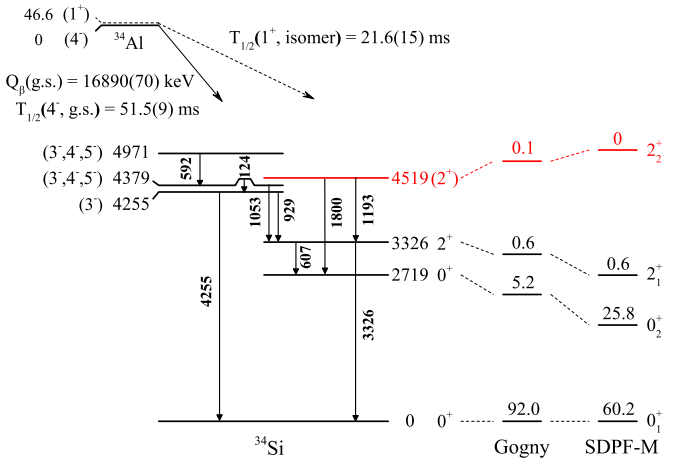

Fig. 3. (Color online). Level scheme for ^{34}Si populated in the β-decay of ^{34}Al along with shell model calculations with the Gogny D1S and the SDPF-M interactions. The experimental level in red is newly determined in the present work. The calculated $0\hbar\omega$ components(%) are labeled on the top of the corresponding levels. Energies are given in keV.

sults are in nice agreement with the experimental data, especially well reproducing the kinks at $Z = 13$. On average, the SDPF-M calculations are closer to the experimental data.

A detailed analysis reveals that the half-lives of these neutron-rich nuclei are very sensitive to the correlation between the wave functions of the parent and the daughter nuclei. The Ne, Na, and Mg nuclei lie inside the "island of inversion" and all have similar dominant intrusive wave functions for the parent and daughter nuclei in the β-decay. Therefore the trend of their half-lives follows the general rule, i.e. increasing when heading towards the β-stability. When approaching the edge of the "island of inversion", as the ground states of Mg isotopes have dominant intrusive wave functions, while the ground states and most of the low-lying excited states in Al isotopes have dominant normal wave functions, the weak correlations between the wave functions of the parent and daughter nuclei result in relative long half-lives of the Mg isotopes. In contrast, when decaying out of the "island of inversion", both Al and Si nuclei have similar dominant normal wave functions, which give rise to the relative short half-lives of Al isotopes. Thus, the kinks occurring at $Z = 13$ can be mainly ascribed to the evolution of the occupation of normal and intruder orbits in the nuclei around the edge of "island of inversion", and therefore considered as a clear sign for the northern boundary of the island. The strong or weak kinks reflect the sharp or gradual structure transition on the northern side of the island, respectively. For example, the sharp structure transition from $\sim 100\%$ intruder configuration of ^{31}Mg [20] to $\sim 100\%$ normal configuration of ^{32}Al [49,50] leads to the strongest kink observed in the $N = 19$ isotonic chain. Detailed β-decay properties certainly will shed more light on the structure transition at the edge of the island. In the following we focus on the detailed β-delayed γ-spectroscopy of ^{34}Al.

Shell model calculations [36,51] predicted that ^{34}Al, as a boundary nucleus of the "island of inversion", should exhibit normal and intruder configurations at similar excitation energies. The coexistence of the normal 4^- ground state and a intruder 1^+ isomeric state results in two β-decay paths, which were first reported in a previous β-decay study [36]. In Ref. [36], a 54.4(5) ms half-life of the 4^- ground state in ^{34}Al was deduced from the β-decay time spectra in coincidence with the 926-keV γ-line in ^{34}Si, while a 26(1) ms half-life of the 1^+ isomer was obtained in coincidence with the positron-annihilation 511-keV γ-line. Since the 511-keV γ-line could also be generated by other sources such as the previously implanted long-lived nuclei and the beam-activated products around, the half-life of the 1^+ isomer may be overestimated. In the more recent experimental works by the same group, a new 25(4) ms half-life of the 1^+ isomer in ^{34}Al was obtained by gating on the γ-lines of ^{34}Si [52] and the excitation energy of the 1^+ isomer was found to be 46.6 keV [53]. Furthermore, with the detection of e^+e^- pairs, the excited energy of the long-predicted 0^+_2 state [54–57] in ^{34}Si was determined and a quadrupole deformation $\beta \sim 0.29$ was extracted for this 0^+_2 state, which coexists with the spherical ground state in ^{34}Si [36].

In the present work, both two β-decay paths are observed (shown in Fig. 3). All the previously reported γ transitions following the β-decay from the 4^- ground state in ^{34}Al [36,58,59] are confirmed here. Gating on the 929-keV transition, the β correlated decay curve yields a half-life of 51.5(9) ms, which is a little smaller than the previously reported value of 54.4(5) ms [36]. In the previous experiment [36], the ^{34}Al nucleus is produced in the fragmentation of a 77.5 MeV/nucleon ^{36}S beam on a 240 mg/cm^2 ^{9}Be target. It is well known that projectile fragmentation can produce fragments in not only ground states but also isomeric states. The proportion of isomeric to ground states population varies greatly with the projectile-fragment combination as well as the incident energy and other experimental conditions. Thus, it would be interesting to figure out the origin of this difference in half-life in a future experiment.

For the decay path from the 1^+ isomer in ^{34}Al, as shown in Fig. 4, due to the combination of a high γ-detection efficiency and a low background level, a γ line at 1193 keV is found to be coincident with the 3326-keV γ ray ($2^+_1 \rightarrow 0^+_1$). This 1193-keV γ line has been observed in several previous experiments [52, 59–63]. Based on the observed coincidence between the 1193- and 3326-keV transitions, a level at 4519 keV was established without spin-parity assignment [52,61,62]. The coincidence between the 1193- and 3326-keV transitions as well as the observation of a 1800-keV deexcited γ-ray transition from the 4519-keV state to the 0^+_2 state at 2719 keV in the present work further confirms the 4519-keV level reported in Refs. [52,61,62]. Gating on

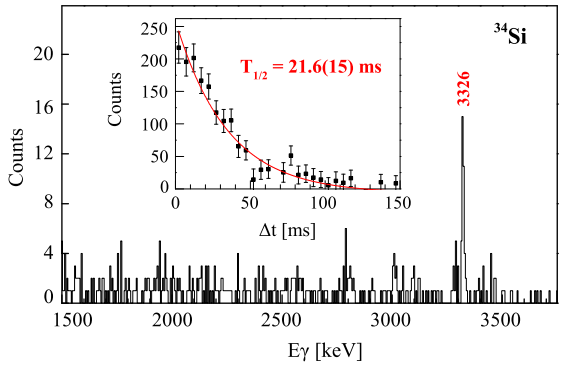

Fig. 4. (Color online). The fragment-β-γ-γ coincidences for ^{34}Al decay gating on 1193-keV γ line. Inset: Decay curve gating on the 1193-keV γ line.

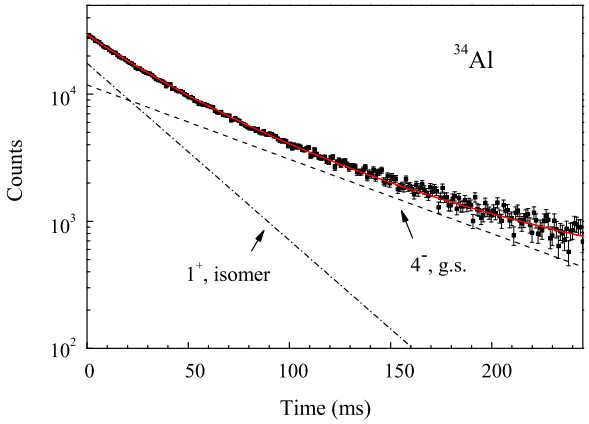

Fig. 5. (Color online). Fitted inclusive decay curve for ^{34}Al. Red solid line: the total decay curve; Dashed line: decay curve of the 4^- ground state; Dot-dashed line: decay curve of the 1^+ isomeric state. Decay contributions from daughter and granddaughter nuclei (not shown in the figure) have been taken into consideration.

the 1193-keV transition, the β correlated decay curve (inset of Fig. 4) yields a half-life of 21.6(15) ms, which is consistent with the more recently reported half-life of 25(4) ms for the 1^+ isomer in ^{34}Al [52]. As no other strong γ-rays are observed to be coincident with the 1193-keV γ ray, the consistence of half-life indicates that this 4519-keV level mainly results from a direct population by the β-decay of the 1^+ isomer in ^{34}Al.

In order to deduce the direct β-decay branching ratio and $\log ft$ value to this 4519-keV state, the total number of β-decay events of the 1^+ isomer is estimated. Using a χ^2 minimization procedure, the inclusive β-decay curve of ^{34}Al, where two components are evident as shown in Fig. 5, was fitted with the measured half-lives of the 1^+ isomeric state and the 4^- ground state, and the β-decay event ratio of the 1^+ isomeric state to the 4^- ground state. Eventually, the fit to the inclusive β-decay curve of ^{34}Al results in a total of 6.5×10^5 measured β-decay events from the 1^+ isomer, from which a decay branching ratio of 11.6% and a $\log ft$ value of 4.9 were obtained for the 4519-keV state. The β-decay allowed nature of the $\log ft$ value from the ^{34}Al 1^+ isomer limits the spin-parity of the 4519-keV level to 0^+, 1^+ and 2^+.

To further study the nature of the low-lying positive-parity states in ^{34}Si, calculations using the Gogny D1S and SDPF-M interactions were carried out and the resulting low-lying positive-parity levels with spin-parity $0^+\sim2^+$, as well as the corresponding configurations, are plotted in Fig. 3 in comparison with the experimental results. It can be seen that both the Gogny D1S and SDPF-M calculations give very similar low-lying positive-parity level structures in ^{34}Si. The correspondences of the first three levels (0_1^+, 0_2^+, 2_1^+) in ^{34}Si between experimental results and calculations are rather good. According to previous studies [36,55,56,58,59,64] and the present calculations, the 0_1^+ ground state has a major $0p$-$0h$ normal configuration, whereas the 0_2^+ and 2_1^+ excited states are dominated by the $2p$-$2h$ intruder component. For the 0_1^+ and 0_2^+ states, the SDPF-M interaction predicts a stronger mixing between the $0p$-$0h$ and the $2p$-$2h$ configurations than the Gogny D1S interaction. Above these first three positive-parity levels, both the Gogny D1S and SDPF-M calculations predict a second 2^+ state with a major $2p$-$2h$ intruder component, which was also predicted in Refs. [55,64]. The calculated energy of 2_2^+ state is so close to the experimental 4519 keV state that this state can be identified. Furthermore, since the 1^+ isomer in ^{34}Al is known to have an intruder $\pi(d_{5/2})^1\otimes\nu(f_{7/2})^2(d_{3/2})^{-1}$ $2p$-$1h$ configuration [36,51], the 0^+ and 2^+ states in ^{34}Si with a $2p$-$2h$ configuration are easily populated by the β-decay of this 1^+ isomer through the conversion of a neutron $d_{3/2}$ into a proton $d_{5/2}$. Compared to the experimental value of 4.9 for the $\log ft$ value to this 4519 keV level, the present calculations yield a value of 4.7 with the Gogny interaction and 5.0 with the SDPF-M interaction. Thus, on the basis of β-decay selection rules and by comparison to shell model calculations, the spin-parity value 2^+ is assigned to the state at 4519 keV with a dominant $2p$-$2h$ intruder component. A 2^+ level at 5330 keV, which was observed in the ^{34}P(^{7}Li, ^{7}Be)^{34}Si experiment and assumed to have a dominant $0p$-$0h$ character [63], is not observed in the present experiment. This can be understood in terms of the weak correlation between the wave functions of the 1^+ isomeric state in ^{34}Al and the 2^+ state at 5330 keV in ^{34}Si.

In Ref. [36], the 0_2^+ and 2_1^+ states with $2p$-$2h$ configurations have been identified to be the members of an excited deformed band above the spherical ground state in ^{34}Si. Two decades ago, Otsuka, based shell model calculations [23], suggested a γ-unstable structure in this region, which has not been observed to date. Of course, it is hard to distinguish experimentally between an axially symmetric and a triaxial minimum if the energy surface is shallow in γ-direction. Here, according to the energetics and the similar dominant intruder configuration as the 2_1^+ state, the newly determined 2_2^+ state at 4519 keV in ^{34}Si shows a level pattern typical for a γ-unstable deformation. It is most likely the band head of a quasi-γ band. Without considering the effects of mixing between the normal 0_1^+ state and the intruder 0_2^+ state, the experimental $E(2_2^+)/E(2_1^+)$ energy ratio (relative to the 0_2^+ state) of 3.0 results, with the Davydov–Filippov model [65], in an empirical triaxial value of $\gamma\sim22^\circ$ and, therefore, displays a prominent signature of triaxiality.

One intriguing result is that a clear γ-unstable structure based on this 2_2^+ state is also predicted by both the Gogny D1S and the SDPF-M interaction. Fig. 6 displays the spectra of ^{34}Si and the corresponding transition probabilities calculated with the two interactions. The resulting $B(E2;2_1^+\rightarrow0_1^+)$ and $B(E2;2_1^+\rightarrow0_2^+)$ values with both interactions reproduce well the experimental values of 17(7) and 61(40) e^2fm^4 [36], respectively, while the calculated $E(2_2^+)/E(2_1^+)$ ratios of 3.3 by the Gogny D1S interaction and 3.5 by the SDPF-M interaction, are a bit larger than the experimental value of 3.0. In the neighboring Si isotopes, significant triaxiality has been clearly shown in potential energy surface (PES) calculations [25,26]. We further examine the PES in the β–γ plane for ^{34}Si by constrained triaxial covariant density functional theory (CDFT) [66,67] using the point-coupling energy density functional PC-PK1 [68]. It is found that in addition to the spherical minimum, a second minimum appears at $\beta\sim0.31$. It is rather soft in γ direction with a long valley from $\sim30^\circ$ to 60° and it is found to be a $2p$-$2h$ excitation with respect to the normal ground state. The pronounced γ softness of this second minimum may lead to the

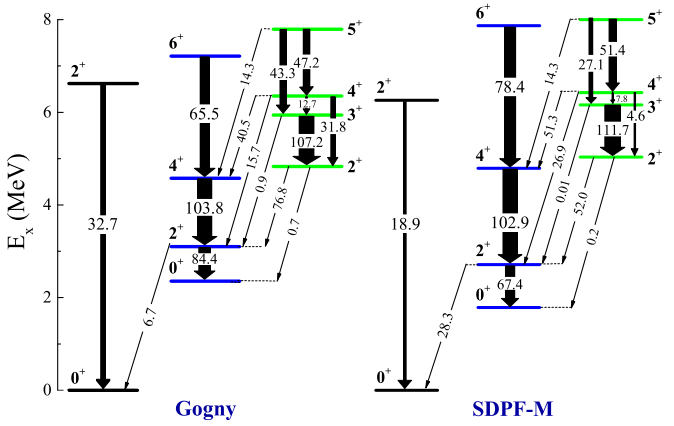

Fig. 6. (Color online). The calculated low-lying energy spectra (in MeV) and $B(E2)$ values (in $e^2\text{fm}^4$) of ^{34}Si by Gogny D1S and SDPF-M interactions.

occurrence of a low-lying γ-vibrational structure with a dominant $2p$-$2h$ configuration in ^{34}Si.

In summary, β-decay studies of neutron-rich nuclei in and around the "island of inversion" have been performed. The observation of the conspicuous kinks of half-lives at $Z = 13$ combined with the observation of a γ-unstable structure in ^{34}Si provide a comprehensive picture of the structure transition across the northern boundary of the island. At present, besides the "island of inversion" around $N = 20$, several other islands have been suggested in the nuclear chart [69] where the picture of the traditional magic numbers may break down. Thus, extending the systematic investigations of the β-decay properties to this archipelago of magic number breaking will be meaningful.

Acknowledgements

R. Han thanks Prof. B.A. Brown for valuable suggestions. C.X. Yuan thanks Profs. Y. Utsuno and T. Otsuka for fruitful discussions. We are grateful to Prof. P. Ring for a critical reading of the manuscript. We would like to acknowledge the staff of HIRFL for providing the ^{40}Ar primary beam and the staff of RIBLL for all kinds of assistance. This work was supported by the Natural Science Foundation of China under Grants No. 11575006, No. 11675003, No. 11375017, No. 11235001, No. 11335002, No. 11375015, No. 11320101004, No. 11461141002, the China Postdoctoral Science Foundation under Grants No. 2015M580007 and No. 2016T90007, and the Chinese Major State Basic Research Development Program under Grant No. 2013CB834400.

References

[1] M.G. Mayer, Phys. Rev. 75 (1949) 1969.
[2] O. Haxel, J.H.D. Jensen, H.E. Suess, Phys. Rev. 75 (1949) 1766.
[3] C. Thibault, et al., Phys. Rev. C 12 (1975) 644.
[4] T. Motobayashi, et al., Phys. Lett. B 346 (1995) 9.
[5] C. Détraz, et al., Phys. Rev. C 19 (1979) 164.
[6] Y. Yanagisawa, et al., Phys. Lett. B 566 (2003) 84.
[7] G. Huber, et al., Phys. Rev. C 18 (1978) 2342.
[8] D. Guillemaud-Mueller, et al., Nucl. Phys. A 426 (1984) 37.
[9] E.K. Warburton, J.A. Becker, B.A. Brown, Phys. Rev. C 41 (1990) 1147.
[10] T. Otsuka, et al., Phys. Rev. Lett. 87 (2001) 082502.
[11] T. Otsuka, et al., Phys. Rev. Lett. 95 (2005) 232502.
[12] T. Otsuka, T. Matsuo, D. Abe, Phys. Rev. Lett. 97 (2006) 162501.
[13] T. Otsuka, et al., Phys. Rev. Lett. 104 (2010) 012501.
[14] L. Gaudefroy, et al., Phys. Rev. Lett. 109 (2012) 202503.
[15] J.R. Terry, et al., Phys. Lett. B 640 (2006) 86.
[16] V. Tripathi, et al., Phys. Rev. Lett. 94 (2005) 162501.
[17] M. Seidlitz, et al., Phys. Rev. C 89 (2014) 024309.
[18] V. Tripathi, et al., Phys. Rev. C 76 (2007) 021301.
[19] M. Petri, et al., Phys. Lett. B 748 (2015) 173.
[20] G. Neyens, et al., Phys. Rev. Lett. 94 (2005) 022501.
[21] A. Gade, et al., Phys. Rev. C 83 (2011) 044305.
[22] A. Gade, et al., Phys. Rev. Lett. 99 (2007) 072502.
[23] T. Otsuka, Nucl. Phys. A 616 (1997) 406.
[24] N. Hinohara, et al., Phys. Rev. C 84 (2011) 061302.
[25] N. Pillet, et al., Phys. Rev. C 85 (2012) 044315.
[26] Y. Utsuno, et al., Phys. Rev. C 86 (2012) 051301.
[27] G.X. Dong, X.B. Wang, S.Y. Yu, Sci. China, Phys. Mech. Astron. 58 (2015) 112004.
[28] J.M. Yao, et al., Phys. Rev. C 79 (2009) 044312.
[29] M. Borrajo, T.R. Rodríguez, J.L. Egido, Phys. Lett. B 746 (2015) 341.
[30] T. Sumi, et al., Phys. Rev. C 85 (2012) 064613.
[31] Z. Sun, et al., Nucl. Instrum. Methods A 503 (2003) 496.
[32] Z.H. Li, et al., Phys. Rev. C 72 (2005) 064327.
[33] Z.H. Li, et al., Phys. Rev. C 80 (2009) 054315.
[34] C. He, et al., Nucl. Instrum. Methods A 747 (2014) 52.
[35] National Nuclear Data Center Evaluated Nuclear Structure Data File, http://www.nndc.bnl.gov/ensdf/.
[36] F. Rotaru, et al., Phys. Rev. Lett. 109 (2012) 092503.
[37] B.A. Brown, et al., NUSHELLX@MSU, http://www.nscl.msu.edu/~brown/resources/resources.html.
[38] W.D.M. Rae, NUSHELLX, http://www.garsington.eclipse.co.uk/.
[39] J. Berger, M. Girod, D. Gogny, Comput. Phys. Commun. 63 (1991) 365.
[40] J. Berger, M. Girod, D. Gogny, Nucl. Phys. A 502 (1989) 85.
[41] J. Dechargé, D. Gogny, Phys. Rev. C 21 (1980) 1568.
[42] W.G. Jiang, et al., in preparation.
[43] Y. Utsuno, et al., Phys. Rev. C 60 (1999) 054315.
[44] Y. Utsuno, et al., Phys. Rev. C 70 (2004) 044307.
[45] B.A. Brown, B.H. Wildenthal, Annu. Rev. Nucl. Part. Sci. 38 (1988) 29.
[46] T. Kuo, G. Brown, Nucl. Phys. A 114 (1968) 241.
[47] D. Millener, D. Kurath, Nucl. Phys. A 255 (1975) 315.
[48] W.G. Jiang, et al., Sci. China, Phys. Mech. Astron. 60 (2017) 082011.
[49] H. Ueno, et al., Phys. Lett. B 615 (2005) 186.
[50] P. Himpe, et al., Phys. Lett. B 643 (2006) 257.
[51] P. Himpe, et al., Phys. Lett. B 658 (2008) 203.
[52] R. Lică, et al., AIP Conf. Proc. 1645 (2015) 363.
[53] R. Lică, et al., Phys. Rev. C 95 (2017) 021301.
[54] N. Fukunishi, T. Otsuka, T. Sebe, Phys. Lett. B 296 (1992) 279.
[55] R.W. Ibbotson, et al., Phys. Rev. Lett. 80 (1998) 2081.
[56] E. Caurier, et al., Phys. Rev. C 58 (1998) 2033.
[57] T. Otsuka, et al., Prog. Part. Nucl. Phys. 47 (2001) 319.
[58] P. Baumann, et al., Phys. Lett. B 228 (1989) 458.
[59] S. Nummela, et al., Phys. Rev. C 63 (2001) 044316.
[60] J. Enders, et al., Phys. Rev. C 65 (2002) 034318.
[61] N. Iwasa, et al., Phys. Rev. C 67 (2003) 064315.
[62] S. Paschalis, et al., J. Phys. Conf. Ser. 312 (2011) 092050.
[63] R.G.T. Zegers, et al., Phys. Rev. Lett. 104 (2010) 212504.
[64] Y. Utsuno, et al., Phys. Rev. C 64 (2001) 011301.
[65] A. Davydov, G. Filippov, Nucl. Phys. 8 (1958) 237.
[66] J. Meng, et al., Phys. Rev. C 73 (2006) 037303.
[67] J. Meng, Relativistic Density Functional for Nuclear Structure, World Scientific, Singapore, 2016.
[68] P.W. Zhao, et al., Phys. Rev. C 82 (2010) 054319.
[69] B.A. Brown, Physics 3 (2010) 104.